JOURNAL OF MATERIALS SCIENCE 30 (1995) 2694–2700

Characterization of gel-grown neodymium heptamolybdate crystals

SUSHMA BHAT, P. N. KOTRU
Department of Physics, University of Jammu, Jammu 180001, India

Neodymium heptamolybdate crystals grown from silica gels [1] are characterized employing energy dispersine X-ray analysis, X-ray and electron diffraction, infra-red spectroscopy, optical microscopy and scanning electron microscopy techniques and the results obtained are presented. The crystals are established to have the composition $Nd_2Mo_7O_{24}27H_2O$. The results of electron diffraction studies indicate the material to be thermally unstable. The crystals growing within the gel medium exhibit varied morphologies including square and octagonal platelets, cuboids, multifaceted crystals, coalesced and aggregated forms and spherulites. The spherulitic morphology is shown to arise due to crystallites adhering in a spherical envelope and are not as a result of crystal fibres radiating out from a centrally located common nucleus. The morphology of the building blocks of the crust at the gel reactant interface is discussed.

1. Introduction

A number of workers [2–33] have dealt with the characterization of gel-grown materials. Some work on low- and high-temperature grown rare-earth molybdates having a general formula $R_2(MoO_4)_3$ is also available in the literature [34–39]. However, to the best of our knowledge, there is no literature available on characterization of rare-earth heptamolybdates grown by any technique. In this paper, the results obtained by various characterizing techniques such as energy dispersive X-ray analysis (EDAX), X-ray and electron diffraction (XRD and ED), infra-red spectroscopy (IR), optical microscopy (OM) and scanning electron microscopy (SEM) are presented.

2. Experimental

The growth of pure Nd heptamolybdate crystals was achieved using the system $Nd(NO_3)_3$–MoO_3–NH_4OH–HNO_3–Na_2SiO_3 [1]. For identification of various constituents of the crystals and establishment of exact stoichiometry, qualitative and quantitative elemental analysis was carried out by using an EDAX unit attached to a SEM model JSM-25 S JEOL made in Japan. A Phillips X-ray powder diffractometer (model Pw 1350) with nickel filtered CuK_α radiation (30 kV, 15 mA) was used to obtain powder diffraction patterns of neodymium heptamolybdate. The instrument was set for a scanning speed of 2° in 2θ min and rate meter and chart speed was maintained constant. The 2θ, intensity and d values (given in Table II) were computed from the diffractogram. The electron diffraction patterns for Nd heptamolybdates were recorded on a TEM, model Phillips EM-300 using a 80 kV beam. The I.R. spectrum was recorded in the range 200 to 4000 cm^{-1} on a Perkin Elmer 424 spectrometer, and a Hitachi 370 spectrometer using the KBr pellet technique.

To study the morphological aspects of the grown crystals, they were examined under optical microscopes Neophot-2 (Carl Zeiss) and Aixophot (Zeiss, Germany) and a scanning electron microscope model JEOL, JSM-80. To increase the conductivity of the grown crystals for SEM observations, the crystals were coated with gold using a fine coat ion sputter, JFC-1100, before examining them under the SEM.

3. Results and discussion

3.1. Energy dispersive X-ray analysis

Qualitative and quantitative elemental analysis performed on application of EDAX is as recorded in Fig. 1 and the data compiled in Table I for neodymium heptamolybdate crystals indicate the presence of molybdenum and the corresponding rare-earth (Nd). The exact stoichiometry of the crystals as suggested by the EDAX analysis confirm that the crystals belong to the heptamolybdate series, the exact composition being $Nd_2Mo_7O_{24}27H_2O$ (for neodymium heptamolybdate). The proposed formula fits very well with the experimental results obtained. The proposed composition was further supported by the results of thermoanalytical techniques.

3.2. X-ray and electron diffraction

The X-ray powder diffractogram recorded for pure Nd heptamolybdate is shown in Fig. 2. These traces (intensity versus 2θ) indicate the crystallinity of the grown material. The X-ray diffraction data compiled for these crystals is given in Table II. To the best of the authors' knowledge, the data reported here is entirely

0022–2461

TABLE I Data from EDAX analysis of Nd heptamolybdate crystals

Crystal name with formula	Atomic percentage (at %)				Weight percentage (wt %)			
	Experimental		Calculated		Experimental		Calculated	
	Nd	Mo	Nd	Mo	Nd	Mo	Nd	Mo
Neodymium heptamolybdate $Nd_2Mo_7O_{24}27H_2O$	18	81	21	78	25	75	30	70

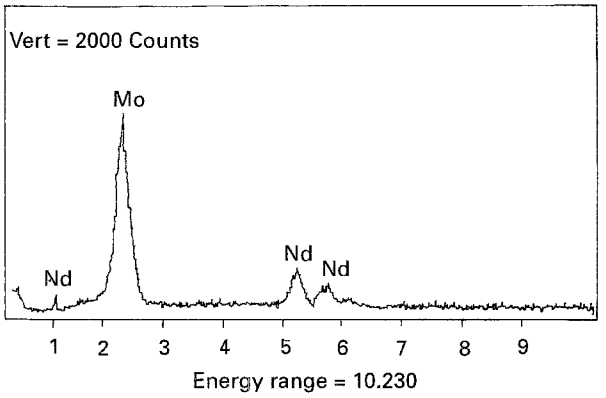

Figure 1 EDAX recorded for $Nd_2Mo_7O_{24}27H_2O$.

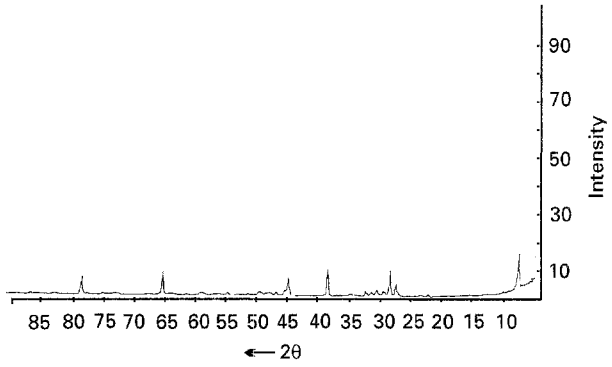

Figure 2 X-ray diffractogram for $Nd_2Mo_7O_{24}27H_2O$.

TABLE II X-ray diffraction data of neodymium heptamolybdate crystals

2θ	*d* (nm)	*I*
7.9	1.11909	27.5
10.8	0.81916	7.5
27.5	0.64867	8.5
28.5	0.62635	15
29.4	0.60758	5.5
30.6	0.58429	6.0
31.4	0.56976	4.7
38.5	0.46765	17
44.8	0.40459	11.7
47.9	0.37981	5.5
54.7	0.33559	3.2
65.2	0.28616	14.5
78.4	0.24394	11.0

new; the X-ray diffraction data on these crystals is not available in the existing literature [40].

It is extremely difficult to record the electron diffraction pattern of the gel-grown crystals of Nd heptamolybdate because the conditions of vacuum and the electron beam heating have an instantaneous effect on their crystallography when they are loaded in the TEM. In spite of the best efforts, the original diffraction pattern of the as-grown crystal could not be recorded because of this problem. However, some intermediate diffraction patterns are presented.

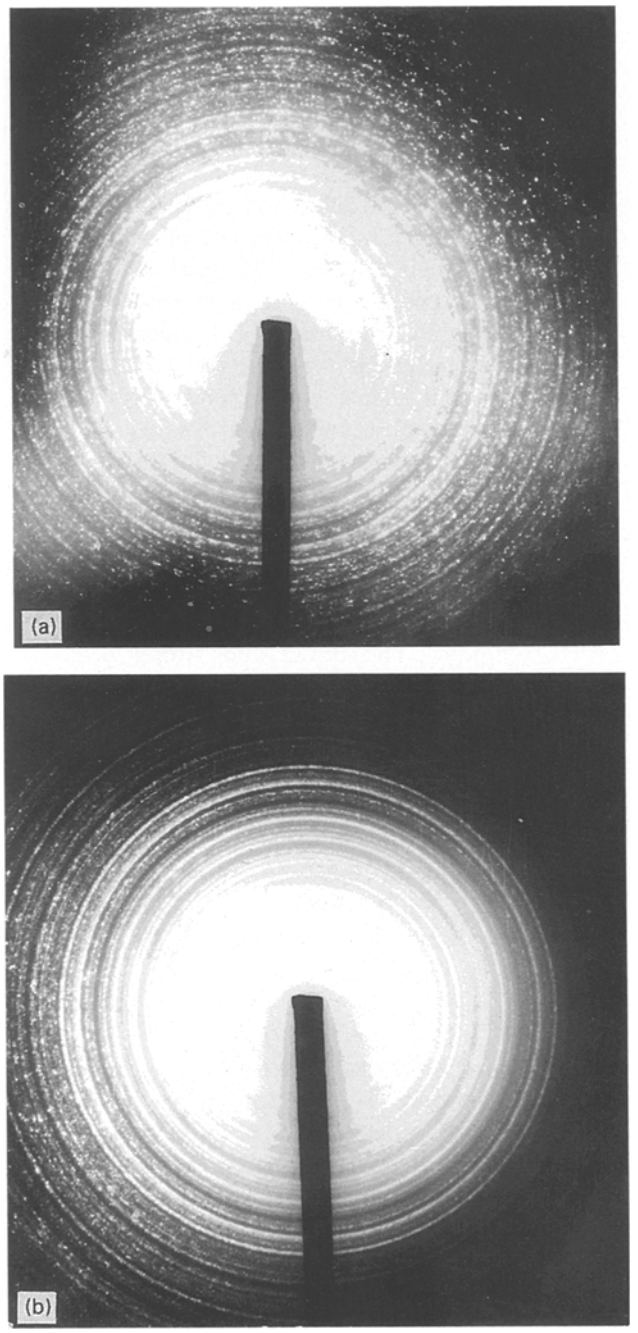

Figure 3 Electron diffraction patterns recorded on pure Nd heptamolybdate immediately (a), and after some time of loading (b), showing transition from better crystallinity to poor cyrstallinity.

Fig. 3a and b are the electron diffraction patterns of Nd heptamolybdate recorded at some intermediate stages of their transformation. Fig. 3a being the one taken at the earliest possible time after allowing the electron beam to be diffracted by the sample, whereas Fig. 3b represents the pattern at a slightly later stage. These recordings show that the material changes from a better crystallinity to a poor one as a consequence of electron beam heating.

Though the single crystallinity of the as-grown material could not be recorded, it is evident that the material is thermally unstable, exhibiting transition from better crystallinity to polycrystallinity, the extent of which depends on the length of time that the electron beam is allowed to pass through the sample. The thermal instability of these crystals is verified from thermoanalytical studies.

The transition in the diffraction patterns, as reported above, is attributed to the presence of water of hydration in the original material. Materials with water of hydration are reported to pose such problems when examined with electron beam [41] which limits the scope of this technique for in-depth studies of such materials. Similar behaviour in respect of crystallinity arising from electron beam heating of some gel-grown crystals has been reported from this laboratory [29–32].

3.3. Infra-red spectroscopy

Fig. 4 is the infra-red spectrum (400–4000 cm^{-1}) recorded for Nd heptamolybdate crystals using the KBr pellet technique. The broad and strong peaks at 3400 cm is due to water and strongly stretching modes of the OH group (ν_1 water-symmetry structure). The peak at 1630 cm^{-1} may be attributed to water (ν_2 water-bending). The peaks occurring at various intervals within the range 400–880 cm^{-1} in the spectrum are due to metal oxygen bonds. It is significant to note that the crystals grown in this laboratory and elsewhere by gel technique have been found to be associated with water of crystallization [12, 21, 27, 33, 29–32, 42–45, 49, 52–55].

3.4. Optical and scanning electron microscopy

The gel growth yields crystals of Nd heptamolybdate in the form of square, octagonal, faceted, cubic and spherulites. Fig. 5a and b are optical micrographs showing various morphologies of these crystals. Distorted spherulitic growth, crystal aggregates, coalesced and twinned crystals can also be observed. Fig. 5c shows some of the crystals of Fig. 5b at a higher magnification illustrating such morphologies.

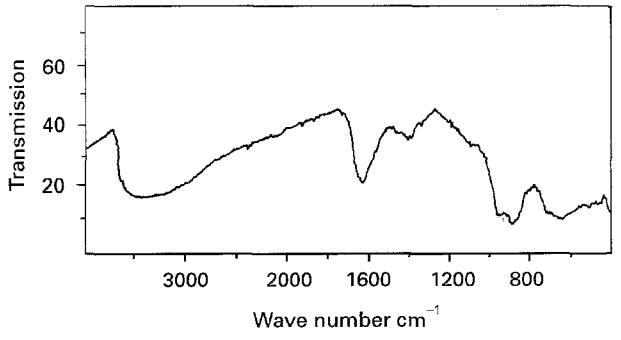

Figure 4 IR Spectrum for $Nd_2Mo_7O_{24}27H_2O$.

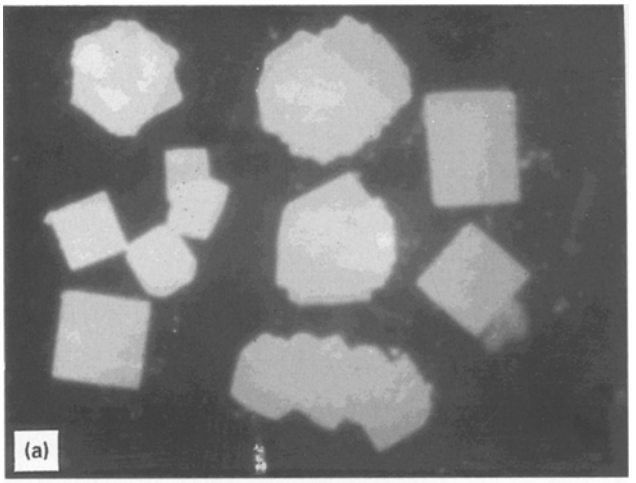

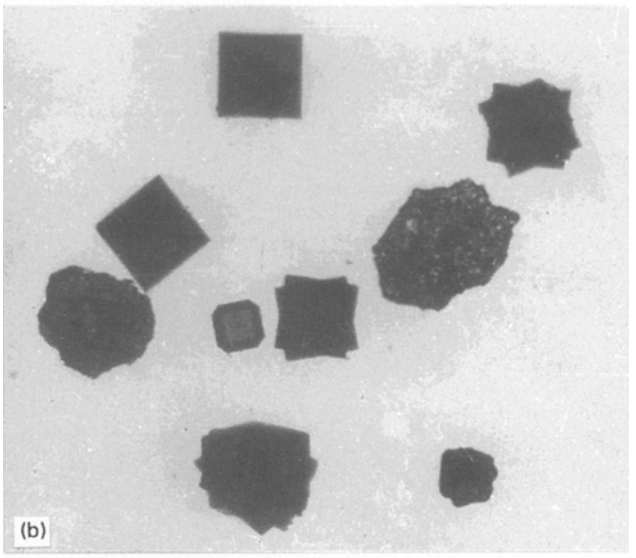

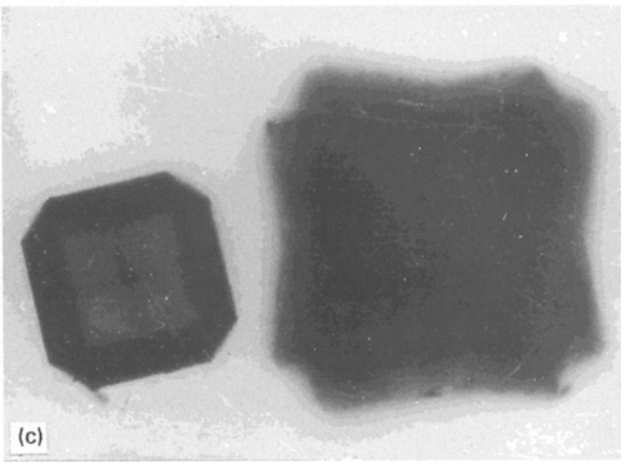

Figure 5 a, b. Optical micrographs showing varied morphology of gel grown Nd heptamolybdate crystals, (c) some of the crystals of (b) at a higher magnification showing octagonal faceted single crystal and a twinned crystal.

The crystals described above are formed somewhere well within the gel medium. However, an instant reaction at the gel-reactant interface leads to the formation of a crust composed of a large number of crystallites. Fig. 6a is a scanning electron micrograph showing such a crust formation of Nd heptamolybdate. Fig. 6(b) shows a region of the crust, at a higher magnification, as observed through an SEM. It clearly shows that the crust is composed of small crystallites having similar morphology to those shown in Fig. 5a and b. Each crystallite appears to be a single crystal. EDAX scanned over the whole crust reveals the same neodymium and molybdenum content as is observed in the case of single crystals. One more type of crust formation is shown in Fig. 7a, while Fig. 7b shows that this crust too is a collection of small single crystallites randomly oriented within the crust.

In order to study the micro- and macro-morphology of the crystals shown in Fig. 5a and b, some of them were examined under an SEM. Fig. 8 a, b and c show some of these crystals at a higher magnification as viewed through an SEM. Fig. 8a reveals that the crystal is faceted (with six faces) and its surfaces are more or less planar. The top and bottom surfaces of this crystal are almost square. Fig. 8b is a crystal with a slightly modified morphology having more or less a trapezoid form. Here also the surfaces of each face are planar. An octagonal-shaped crystal exhibits more faces as illustrated in Fig. 8c. Cracks can be observed in all the three crystals of Fig. 8a, b and c. It may be noted that these cracks develop as a result of loading them in vacuum (while gold plating) coupled with electron beam heating. This effect is a result of the fact that these crystals carry 27 waters of hydration as has been verified by thermoanalytical techniques. It is quite interesting to note that these cracks do not follow any crystallographic direction and may arise as a result of water leaving the crystal.

Gel growth is reported to have resulted in spherulitic growth of a large number of materials [4, 46–57]. Spherulitic morphology is an interesting problem in crystal growth. Various workers have, therefore, made attempts to explain the mechanism of spherulitic crystallization. A treatment by Keith and Padden [58] has presented a phenomenological theory of spherulitic crystallization. Bolotov and Muravea [48] have explained that a selenium spherulite develops from a single crystal nucleus drawn out in a direction perpendicular to the c-axis lying in the plane of the crystal, the curving of the lattice being as a result of surface tension forces acting on different faces. According to spherulitic mechanism proposed by McCauley and Roy [59], the nucleus is a tiny prismatic crystal, then owing to contamination there is a subsequent radial growth of acicular crystals. Kotru and Raina [54] investigated the internal

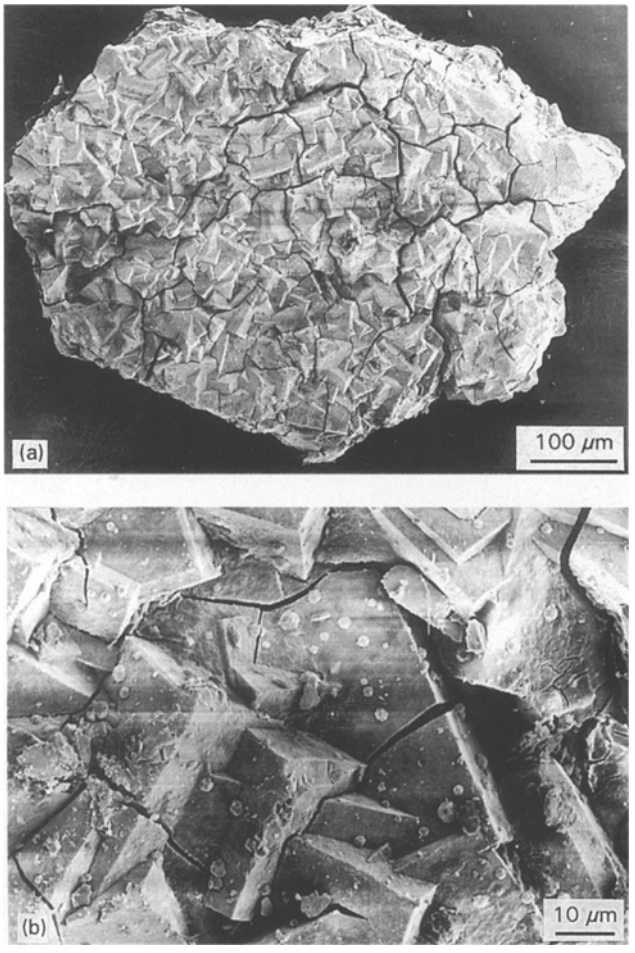

Figure 6 (a) Scanning electron micrograph of a crust of Nd heptamolybdate formed at the gel reactant interface. (b) A region of (a) at a higher magnification, revealing the morphology of the crystallites building the crust.

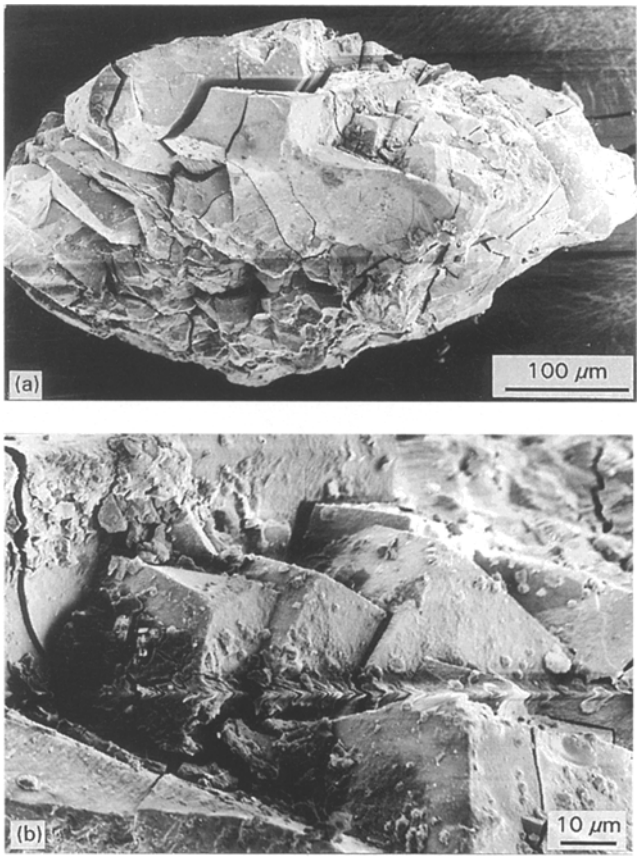

Figure 7 (a) Scanning electron micrograph showing the upper surface of a crust of Nd heptamolybdate. (b) The encircled portion of (a) at a higher magnification revealing the morphology of crystals at a very early stage of growth.

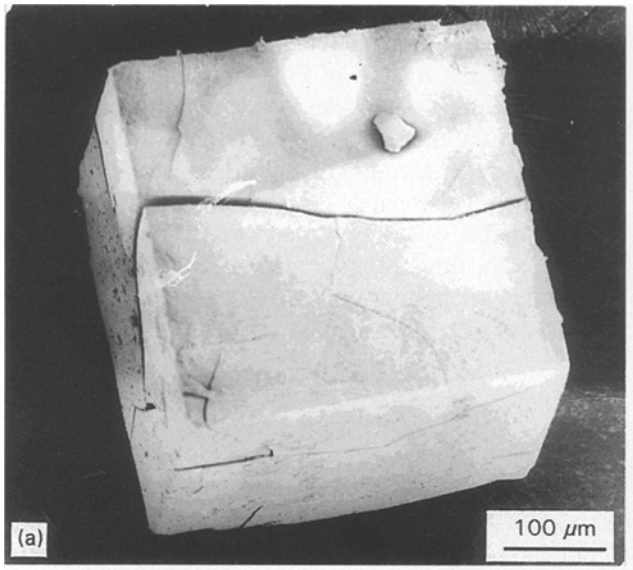

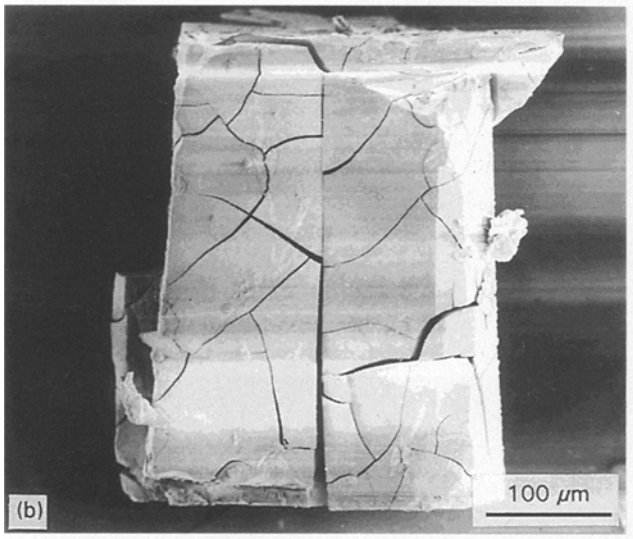

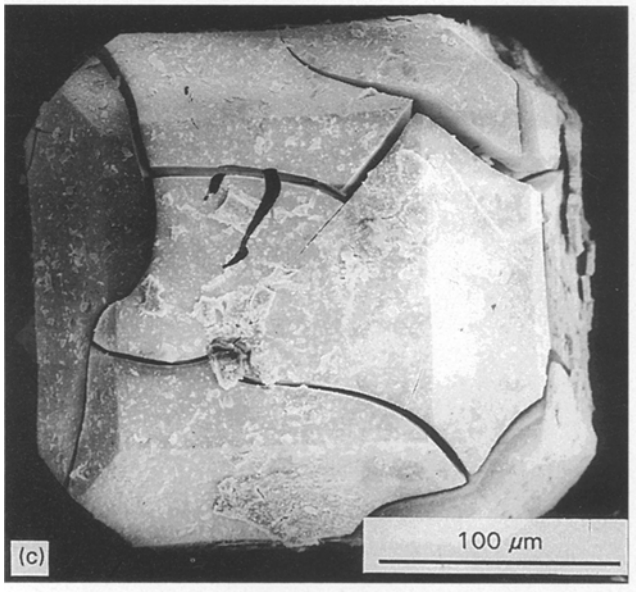

Figure 8 Scanning electron micrographs illustrating some different morphologies assumed by gel-grown Nd heptamolybdate crystals. (a) Faceted crystal with plane habit faces. (b) Faceted crystal with more or less a trapezioid shape. (c) Multifaceted octagonal crystal.

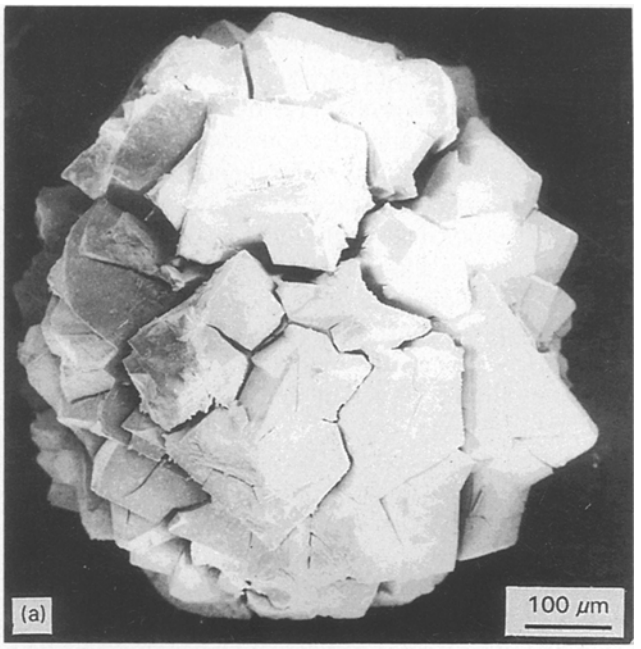

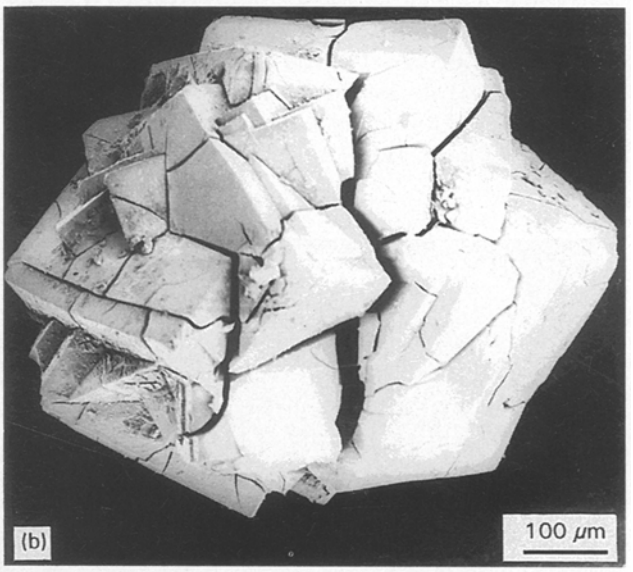

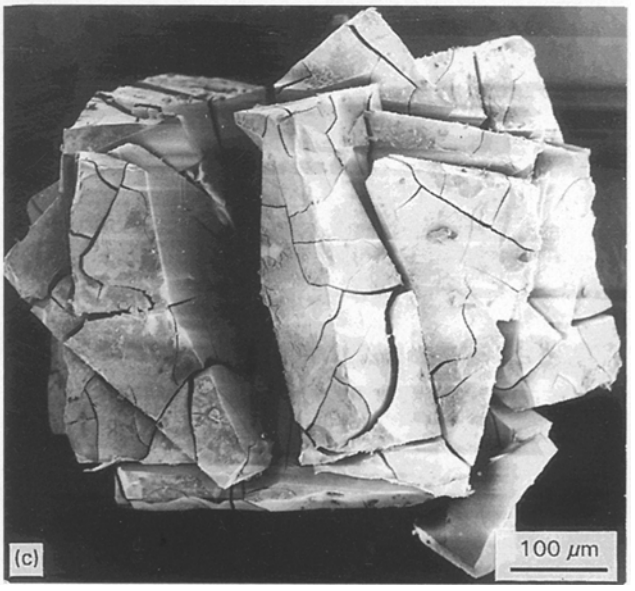

Figure 9 Scanning electron micrographs showing different forms of spherulitic morphologies of gel-grown Nd heptamolybdate crystals. Note that in none of these cases the origin is due to radiating fibres from a common or multiple nuclei.

structure of Nd, Dy and Di tartrate spherulites and suggested a new mechanism of spherulitic formation. According to them, the initial growth is a highly polycrystalline state within a spherical volume which at some later stage of growth offers multiple nuclei for the growth of radially diverging fibres. As such, the fibres radiate from multiple nuclei and not only from a centrally located common nucleus as proposed by Boltov and Muravea [48] and McCauley and Roy [59]. This mechanism of spherulitic formation is supported by the observations reported by Jain [66].

Spherulitic morphology is also exhibited in the gel growth of Nd heptamolybdate as shown in Fig. 5a and b. In order to investigate their mechanism of formation, some of the spherulites were examined under an SEM. Fig. 9a, b and c are the scanning electron micrographs showing various types of spherulites of Nd heptamolybdate. Ignoring the cracks (developed due to gold plating and electron beam heating) one finds the spherulites to be composed of small crystallites in a more or less spherical envelope. Scanning by the EDAX indicates that the individual building blocks of spherulites are Nd heptamolybdates. These are not radiating fibres from a single or a multiple nuclei as reported by earlier workers (see above). Therefore, it is suggested that a spherulitic morphology can also be due to single crystallites joining together in a spherical envelope. The boundaries between the two individual blocks are the weak spots which is amply supported by the observation that they crack preferentially first along the boundaries joining them. However, the cracks later develop along the plane surfaces of individual blocks which also do not bear any crystallographic direction. Fig. 10 shows cracks on the plane surface of an individual block propagated in non-crystallographic directions.

From the above study, it is inferred that the gel-grown Nd heptamolybdate crystals exhibit a variety of morphologies which include nearly square and octagonal platelets, cuboids, multifaceted crystals and spherulites. The crystals grow by a two dimensional nucleation mechanism.

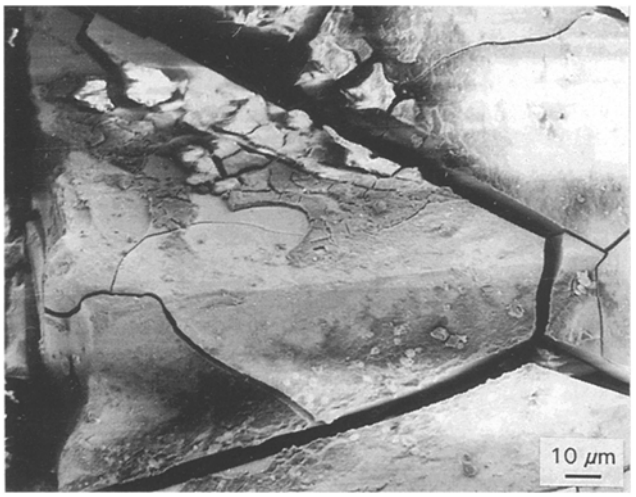

Figure 10 Scanning electron micrographs demonstrating the propagation of vacuum- and electron beam heating-induced cracks bearing no definite crystallographic directions.

4. Conclusions

1. The qualitative and quantitative elemental analysis, employing the EDAX technique, confirm the growth of Nd heptamolybdate crystals from silica gel, using the system $Nd(NO_3)_3$–MoO_3–NH_4OH–HNO_3–Na_2SiO_3; the composition being $Nd_2Mo_7O_{24}27H_2O$.
2. The X-ray diffraction indicates crystallinity of Nd heptamolybdate.
3. The results of infra-red spectroscopy establish the crystals to be hydrated.
4. The optical and scanning electron microscopic studies reveal growth of Nd heptamolybdate crystals which exhibit various morphologies including square and octagonal platelets, cuboids, multifaceted crystals, coalesced and aggregated forms and spherulites.
5. The spherulites arise from a large number of tiny crystallites adhering in a spherical envelope and are definitely not as a result of crystal fibres radiating out from a centrally located common nucleus.
6. The instant reaction between the two reactants at the gel–reactant interface leads to the formation of a crust whose building blocks are tiny crystallites.
7. The results of electron diffraction reveal changes in the diffraction patterns, suggesting transformation from a crystalline pattern to a polycrystalline pattern because of electron beam heating effects. The cracking of crystals while loading samples in a vacuum chamber and during SEM observations suggest that Nd heptamolybdate crystals are thermally unstable; the cracks arising as a result of water leaving the hydrated crystals. This conclusion is further supported by the results of thermoanalytical studies.

References

1. SUSHMA BHAT, M. L. KOUL and P. N. KOTRU, *J. Mat. Sci. Eng. B*, **23** (1994) 73.
2. Z. BLANK, W. BRENNER and Y. OKAMOTO, *Mat. Res. Bull.* **3** (1968) 555.
3. J. W. McCAULEY and H. W. GEHRCHARDT, AMMRC. TR70-13, Army Materials and Mechanics Research Center, Waterton MA (1970).
4. K. NASSSAU, A. S. COPPER, J. W. SHIEVER and B. E. PRESCOTT, *J. Solid State Chem.* **8** (1973) 260.
5. K. SANGWAL, A. R. PATEL, *J. Cryst. Growth* **23** (1974) 282.
6. N. CHAND and G. C. TRIGUNAYAT, *ibid.* **39** (1977) 299.
7. A. R. PATEL and S. K. ARORA, *Kristall Und. Tech.* **13** (1978) 899.
8. M. S. JOSHI and B. T. BHOSKAR, *J. Cryst. Growth* **47** (1979) 654.
9. F. LEFAUCHEUX and M. C. ROBERTS, *ibid.* **47** (1979) 313.
10. C. C. DESAI and J. L. RAI, *ibid.* **53** (1981) 432.
11. D. JAYAKUMMAR and K. S. RAJU, *Bull. Mat. Sci.* **5** (1983) 399.
12. B. WIKTOROWSKA, B. BORECKA and J. KARNIEWICZ, *J. Mat. Sci.* **18** (1983) 416.
13. A. R. PATEL and S. K. ARORA, *ibid.* **11** (1976) 843.
14. *Idem, J. Cryst. Growth* **37** (1977) 343.
15. M. S. JOSHI and A. V. ANTONY, *J. Mat. Sci.* **13** (1978) 939.
16. Z. BONTSCHEWA-MLLADENOVA and G. GEORGIEW, *Monatsh Chem.* **106** (1975) 283.
17. Z. BONCHEVA-MLADENOVA and N. DISHOVSKY, *J. Cryst. Growth* **47** (1979) 82.
18. *Idem, ibid.* **47** (1979) 467.
19. T. SHRIPATHI, H. L. BHAT, P. S. NARAYANAN, *J. Mat. Sci.* **15** (1980) 3095.
20. V. P. BHATT, R. M. PATEL, *J. Cryst. Growth* **53** (1981) 633.

21. G. POLLA, R. F. BAGGIO, E. MANGHI and P. K. DEPERAZZO, *J. Cryst. Growth* **67** (1984) 68.
22. V. SARASWATI, *J. Cryst. Growth Lett.* **83** (1987) 606.
23. S. K. MOHAN LAL and R. BASKARAN, *Cryst. Res. Technol.* **22** (1987) 21.
24. W. BUCHDE and A. LENTZ, *Cryst. Res. Technol.* **22** (1987) 27.
25. W. G. PERDOK and J. CHRISTOFFERSEN, *J. Cryst. Growth* **80** (1987) 149.
26. ROSENDO SANJINES, K. RAVINDRANTHAN, THAMMPI and J. KIWI, *J. Am. Ceram. Soc.* **71** (1988) 512.
27. P. N. KOTRU, N. K. GUPTA, K. K. RAINA and I. B. SHARMA, *J. Mat. Sci.* **21** (1986) 83.
28. P. N. KOTRU, N. K. GUPTA, K. K. RAINA and M. L. KOUL, *Bull. Mat. Sci.* **8** (1986) 547.
29. P. N. KOTRU, K. K. RAINA and M. L. KOUL, *J. Mat. Sci*, **21** (1986) 3933.
30. *Idem., Ind. J Pure Appl. Phys.* **25** (1987) 220.
31. *Idem., J. Mat. Sci. Lett.* **6** (1987) 711.
32. SUSHMA BHAT, MPhil. dissertation, Dept. of Physics, University of Jammu, Jammu (1988).
33. V. MANSOTRA, K. K. RAINA, P. N. KOTRU and M. L. KOUL, *J. Mat. Sci.* **26** (1991) 6729
34. K. V. KURIEN, V. K. VAIDYAN and M. A. ITTYACHEN, *Proc. Ind. Acad. Sci. (Chem. Sci.)* **92** (1983) 233.
35. *Idem., ibid.* **2** (1983) 261.
36. L. H. BRIXNER, *J. Cryst. Growth* **18** (1973) 297.
37. K. NASSAU, H. J. LEVINSTEIN and G. M. LOIACONO, *J. Phys. Chem. Solids* **26** (1965) 1805.
38. P. B. JAMIESON, S. C. ABRAHAMS and J. L. BERNSTEIN, *J. Chem. Phys.* **50** (1969) 86.
39. H. J. BORCHARDT and P. E. BIERSTEDT, *J. Appl. Phys.* **38** (1976) 2057.
40. ASTM cards
41. M. H. LORENTTO, "Physico-chemical methods of mineral analysis", edited by A. W. Nichol (Plenum Press, New York, 1975) 324.
42. P. N. KOTRU, N. K. GUPTA and K. K. RAINA, *J. Mat. Sci.* **21** (1986) 90.
43. S. NARAYAN KALKURA and S. DEVANARAYANAN, *J. Cryst. Growth* **83** (1987) 446.
44. M. OHIA and M. TSU TSUMI, *ibid.* **56** (1982) 652.
45. M. PRIETO, C. VIEDMA, V. LOPEZ-ACEVEDO, J. L. MARTIN-VIVALDI and S. LOPEZ-ANDRES, *ibid.* **92** (1986) 61.
46. H. W. MORCE, C. H. WARREN, J. D. DONNAY, *Amer. J. Sci.* **23** (1932) 421.
47. *Idem. Amer. Mineralogist* **21** (1936) 391.
48. I. E. BOLOTOV and E. A. MURAVEA, "Growth and imperfections of metallic crystals", edited by D. E. Ovsienko (Consultants Bureau, New York, 1968) p. 76.
49. P. N. KOTRU, K. K. RAINA and N. K. GUPTA, *Cryst. Res. Tech.* **22** (1987) 177.
50. P. N. KOTRU and K. K. RAINA, *J. Mat. Sci. Lett.* **5** (1986) 760.
51. P. N. KOTRU, N. K. GUPTA and K. K. RAINA, *Cryst. Res. Tech.* **21** (1986) 15.
52. V. MANSOTRA, K. K. RAINA and P. N. KOTRU, *J. Mat. Sci.* **26** (1991) 3780.
53. ANIMA JAIN, ASHOK K. RAZDAN and P. N. KOTRU, *Mat. Sci. Eng. B* **8** (1991) 21.
54. P. N. KOTRU and K. K. RAINA, *J. Cryst. Growth* **91** (1988) 221.
55. O. SOHNEL and J. W. MULLER, *ibid.* **60** (1982) 239.
56. A. R. PATEL and S. K. ARORA, *ibid.* **18** (1973) 199.
57. Z. BLANK and W. BRENNER, *J. Cryst. Growth* **11** (1971) 255.
58. M. D. KIETH and F. J. PADDEN, *J. Appl. Phys.* **34** (1963) 2409.
59. J. W. McCAULEY and R. ROY, *Amer. Miner.* **59** (1974) 947.
60. ANIMA JAIN, PhD Thesis, Jammu University, Jammu (1991)

Received 22 October 1993
and accepted 27 July 1994